PREDICTIONS OF TURBULENT HEAT TRANSFER OF SUPER-CRITICAL CARBON DIOXIDE FLOW IN A SQUARE DUCT WITH AN ELLIPTIC-BLENDING SECOND MOMENT CLOSURE

Young Don Choi, Seong Ho Han, Jeong Soo An,
Department of Mechanical Engineering, Korea University,
1, Anam-dong, Sungbuk-ku, Seoul 136-701, Korea
ydchoi@korea.ac.kr, hshengin@korea.ac.kr, anjsoo@korea.ac.kr

Jong Keun Shin
Department of Automotive Engineering, Donghae University,
119, Jiheung-dong, Donghae, Kangwondo 240-713, Korea
jkshin@donghae.ac.kr

ABSTRACT

The present contribution describes the application of elliptic-blending second moment closure to the prediction of gas cooling process of turbulent super-critical carbon dioxide flow in a square cross-sectioned duct. The gas cooling process under super-critical state experiences a drastic change in thermodynamic and transport properties. Thus it induces the extraordinary variations of heat transfer coefficients of the duct walls much different from those of single or two phase flows. Redistributive terms in the Reynolds stress and turbulent heat flux equations are modeled by an elliptic-blending second moment closure in order to represent strongly inhomogeneous effects produced by the presence of walls. The main feature of Durbin's elliptic relaxation model which avoids the need for quasi-homogeneous algebraic models and damping functions for near wall modeling of redistributive terms is maintained by the elliptic-blending second moment closure but it involves only one scalar elliptic equation. Computations were performed for the developing turbulent flow during the cooling process of super-critical carbon dioxide flow in a square duct. The results will be used usefully to establish a new heat transfer coefficient correlation widely applicable to the gas cooler design involving turbulent super-critical carbon dioxide flow.

INTRODUCTION

As the CFC and HCFC refrigerants may cause global warming and ozone depletion, the trans-critical dioxide(R-744) cycle has recently got into spot light as an alternative refrigerant for air conditioners. Carbon dioxide in trans-critical state possesses a high specific heat and excellent thermodynamic and transport properties as a refrigerant. One of the major difference between trans-critical carbon dioxide cycle and convectional cycle is the heat rejection process. The heat rejection process in the trans-critical cycle takes place by cooling the high pressure carbon dioxide gas along a super-critical isobar. During the heat rejection process, the thermo-physical properties of carbon dioxide change drastically, but phase change does not take place. Therefore, the heat rejection process is called a "gas cooling process" instead of condensing process. Correct prediction of heat transfer rate in the gas cooling process has been recognized as the most important factor for the efficient gas cooler design involving carbon dioxide refrigerant.

Various experimental investigations are performed to obtain the heat transfer coefficient correlation that can be efficiently used for the design of gas coolers involved in the trans-critical carbon dioxide cycle. Petukhov et al.[1961], Krasnoshchekov et al.[1970], Pitla et al.[2002], and Petrov and Popov[1985] proposed the heat transfer coefficient correlations for turbulent super-critical carbon dioxide flow in pipes based on their experimental results. However, the proposed correlations are not yet ensured as much as reliable to be used for the gas cooler designs of carbon dioxide air conditioners. That is due to the difficulties in correct measurements of turbulent heat transfer coefficients in the pipes or ducts under various heat flux boundary conditions. Especially, as the carbon dioxide flow approaches to the pseudo-critical point, the turbulent heat transfer process becomes so complex due to many influencing parameters, pressure, temperature, wall heat flux, Reynolds number and compressibility factor, etc. that makes it difficult to extract the reliable heat transfer coefficient correlations from the limited number of data.

The heat transfer coefficient correlation can be determined by solving the governing equations of continuity, momentum and energy. In many respects, establishing the turbulent heat transfer coefficient correlation of super-critical carbon dioxide flow in pipes or ducts by computational means is more efficient than that by experimental means only. A number of first order turbulence closures employing eddy diffusivity model have been introduced to predict the turbulent heat transfer coefficient of super-critical carbon dioxide flows. Although much improvement has been established by introducing the first order turbulence models to predict the turbulent heat transfer of super-critical carbon dioxide flow, the first order closures always

suffer form the eddy diffusivity concept that cannot involve redistributive effects of Reynolds stresses and turbulent heat fluxes. Many researchers try to improve turbulence model by tuning two-equation and algebraic flux model for heat transport. Despite some success, it is still believed that the most reliable prediction methods are those based on the second moment closures. Redistributive terms in the Reynolds stress and turbulent heat flux equations are strongly affected by the inhomogeneity due to the presence of wall. The inhomogeneity effects can be efficiently modeled by elliptic-blending second moment closure. The main feature of Durbin's elliptic relaxation model which avoids the need for quasi-homogeneous algebraic models and damping functions for near wall modeling of redistributive terms is maintained by the elliptic-blending second moment closure but it involves only one scalar elliptic equation.

The objective of the present study is to expand the elliptic operator to the full second moment treatment of heat flux. In the present study the elliptic-blending concept is applied to predict the gas cooling process of turbulent supercritical carbon dioxide flow in a square cross-sectional duct. Computations were performed for the developing turbulent heat transfer of super-critical carbon dioxide flow in a square duct during the heat rejection process.

MATHEMATICAL MODELS

Elliptic-blending equation for turbulent heat flux

A mathematical model of turbulent scalar transport is required for solving the Reynolds-averaged scalar equation. In the second moment closure, the generation term due to mean velocity and scalar gradients can be handled exactly, and this feature should be one of the most attractive advantages when predicting complex flows. The exact transport equation for the scalar flux in a fluid of variable physical properties is given by:

$$\frac{D\overline{u_i\theta}}{Dt} = P_{i\theta} + G_{i\theta} + D^t_{i\theta} + D^\nu_{i\theta} + \Phi^*_{i\theta} - \epsilon_{i\theta} \tag{1}$$

The meaning of the terms in Eq. (1) from left to right are convective transport, generation terms due to scalar gradient, turbulent diffusive transport, viscous diffusive transport, pressure scrambling (temperature- pressure gradient correlation) and molecular dissipation of scalar fluxes. Considering the near-wall behaviour of heat scalar equations, the unclosed terms in Eq. (1) can be modelled as follows. Firstly, the turbulent diffusion term is modelled via the standard gradient transport hypothesis as:

$$D^t_{i\theta} = \frac{\partial}{\partial x_k}\left(C_\theta \overline{u_k u_l}\, T \frac{\partial \overline{u_i\theta}}{\partial x_l} \right) \tag{2}$$

with the coefficient $C_\theta = 0.153$. Contrary to the Reynolds stress model, the molecular diffusion is not of the correct term. The model suggested by Lai & So[1990] is adopted as:

$$D^\nu_{i\theta} = \nu \frac{\partial^2 \overline{u_i\theta}}{\partial x_k^2} + \frac{\alpha - \nu}{n_i + 2} \frac{\partial^2 \overline{u_i\theta}}{\partial x_k^2} \text{(no summation for } i\text{)} \tag{3}$$

In Eq. (3), the n_i means the unit normal to the wall. Exact expressions for the turbulent heat flusx generation terms, $P_{i\theta}$ and $G_{i\theta}$, in Eq. (1) are as follows

$$P_{i\theta} = -\left(\overline{u_i u_j} \frac{\partial T}{\partial x_j} + \overline{u_i\theta} \frac{\partial U_i}{\partial x_j} \right) \tag{4}$$

$$G_{i\theta} = -\beta g_i \overline{\theta^2} \tag{5}$$

where β is the thermal expansion coefficient defined as

$$\beta = -\frac{1}{\rho}\frac{\partial \rho}{\partial T}\bigg|_P \tag{6}$$

Buoyant force induced by local thermal stratifications in the duct flow affects the turbulence structure both through the buoyant generation of turbulence and redistributive terms in the Reynolds stress and turbulent heat scalar equations. The buoyant generation of turbulent scalar flux $G_{i\theta}$ is proportional to thermal expansion coefficient β as shown in the Eq. (5). With regard to ideal gas, as the state equation is represented as $P = \rho RT$, the thermal expansion coefficient is given by $\beta = 1/T$. However, with regard to non-ideal gas, as the state equation becomes to $P = Z\rho RT$, the thermal expansion coefficient changes to

$$\beta = \frac{1}{T} - \frac{dZ}{Z dT} \tag{7}$$

Where Z is compressibility factor that illustrate the departure of a pure substance from the ideal-gas behavior. As the supercritical carbon dioxide flow approaches to the pseudo-critical point, the gradient of compressibility factor increase sharply so that the portion of $dZ/Z/dT$ in the thermal expansion coefficient formulation (7) increases and the ratio of buoyant to shear generations of Reynolds stresses increases sharply.

In order to obtain $\overline{\theta^2}$ in Eq. (5), transport equation $\overline{\theta^2}$ should be solved. The exact transport equation for $\overline{\theta^2}$ is given by

$$\frac{D\overline{\theta^2}}{Dt} = P_{\overline{\theta^2}} + D^t_{\overline{\theta^2}} + D^\nu_{\overline{\theta^2}} - \epsilon_{\overline{\theta^2}} \tag{8}$$

The meaning of the terms in Eq. (8) from the right to right are convective transport, generation term by the mean field, turbulent diffusive transport, molecular diffusive transport and dissipation of scalar fluctuation. Both for the turbulent and laminar diffusion terms, the gradient transport hypothesis are applied as;

$$D_{\overline{\theta^2}}^{t} = \frac{\partial}{\partial x_k}\left(C_\theta \overline{u_k u_\theta}\, T \frac{\partial \overline{\theta^2}}{\partial x_l} \right) \tag{9}$$

$$D_{\overline{\theta^2}}^{\nu} = \alpha\left(\frac{\partial^2 \overline{\theta^2}}{\partial x_k^2} \right) \tag{10}$$

Exact expression for generation by the mean field is given by

$$P_{\overline{\theta^2}} = -2\overline{u_k\theta}\frac{\partial T}{\partial x_k} \tag{11}$$

The dissipation $\epsilon_{\overline{\theta^2}}$ of the fluctuating scalar is determined by the function of the time scale ratio.

$$R = \frac{\epsilon}{k}\frac{\overline{\theta^2}}{\epsilon_{\overline{\theta^2}}} \tag{12}$$

with the coefficient R=0.8

The temperature-pressure gradient correlation term $\Phi_{i\theta}^{*}$ and the dissipation term $\epsilon_{i\theta}$ in Eq. (1) are major sink term and need to be carefully modeled. By following the same approach as for the turbulent stress field, we can express the pressure scrambling and molecular destruction with elliptic equations analogue to elliptic-blending method of Reynolds stress equation.

$$\Phi_{i\theta}^{*} = (1-\psi^2)\Phi_{i\theta}^{w} + \psi^2 \Phi_{i\theta}^{h} \tag{13}$$

$$\epsilon_{i\theta} = (1-\psi^2)\epsilon_{i\theta}^{w} + \psi^2 \epsilon_{i\theta}^{h} \tag{14}$$

In the above models, the ellipticity of the models is preserved by solving an elliptic differential equation as

$$\psi - L^2 \nabla^2 \psi = 1 \tag{15}$$

with the boundary conditions $\psi = 0$ at the wall (Thielen *et al.*, 2005). For $\Phi_{i\theta}^{h}$ any known quasi-homogeneous model can be adopted and the most general model (Durbin, 1993) is chosen in the present study.

$$\Phi_{i\theta}^{h} = -C_{1\theta}\frac{\epsilon}{k}\overline{u_i\theta} + C_{2\theta}\overline{u_i u_j}\frac{\partial \Theta}{\partial x_j} + C_{3\theta}\overline{u_j\theta}\frac{\partial U_i}{\partial x_j} \tag{16}$$

with $C_{1\theta} = 2.5$, $C_{2\theta} = 0.45$ and $C_{3\theta} = 0.0$. Because the dissipation term in the high Reynolds number region has been assumed to be isotropic, we let

$$\epsilon_{i\theta}^{h} = 0. \tag{17}$$

To impose the limiting wall behaviour of turbulent heat fluxes, $\Phi_{i\theta}^{w}$ and $\epsilon_{i\theta}^{w}$ can be modeled in such a way that it will approach its asymptotic value near the wall.

$$\Phi_{i\theta}^{w} = -\frac{\epsilon}{k}\overline{u_k\theta}\, n_k n_i \tag{18}$$

$$\epsilon_{i\theta}^{w} = \frac{1}{2}\left(1 + \frac{1}{\mathrm{Pr}}\right)\frac{\epsilon}{k}\left(\overline{u_i\theta} + \overline{u_k\theta} n_k n_i\right) \tag{19}$$

For the reproduction of the limiting wall behaviour of $\Phi_{i\theta}^{w}$ and $\epsilon_{i\theta}^{w}$, the wall-normal vector is used. However, the use of a wall-normal vector must be avoided, since such a quantity is often not well defined in complex geometries. Therefore, in the present work, a new concept suggested by Thielen *et al.*[2005] is adopted as:

$$\mathbf{n} = \frac{\nabla \psi}{\| \nabla \psi \|} \tag{20}$$

NUMERICAL TREATMENT

Heat flux boundary and flow conditions

The gas cooling processes of turbulent super-critical carbon dioxide flows in a square duct were solved for the two kinds of heat flux boundary conditions. One is the rejection of constant heat flux from all around the duct wall and the other is the rejection of constant heat flux only from the upper and lower walls. Fig. 1 shows the two heat flux boundary conditions. At all computations, the Reynolds number based on bulk mean velocity, density, viscosity and hydraulic diameter is fixed to 10^5 and bulk mean temperature to 100℃ at the duct inlet. Duct inlet pressure is changed to 7.353MPa and 10MPa. Isobar of R=7.353MPa passes through critical point. For each duct inlet pressure, three kinds of wall heat fluxes -10,000W/m^2, -20,000W/m^2 and -40,000W/m^2 are applied to the wall. The heat transfer computations are continued until the bulk mean temperature of supercritical carbon dioxide decreases to about 30℃.

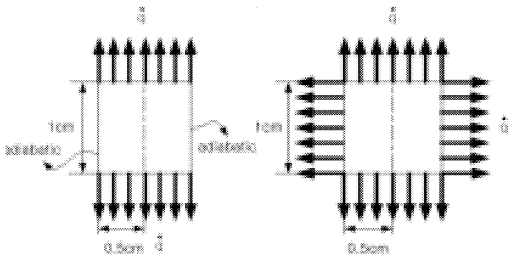

(a) (b)

Fig. 1 Heat flux boundary condition for a square duct.
(a) constant heat rejection from upper and lower walls
(b) constant heat rejection from all around the wall

Calibration of new heat flux model

In order to calibrate the present heat flux model, the velocity field variables are supplied from DNS data and the differential equations only for the mean temperature and the scalar flux are solved by the present calculations with constant wall heat flux conditions

respectively. Therefore, any failure in the present models can be attributed to the heat flux modeling. Two Reynolds number of Re_τ=180 and 395 are calculated, where Re_τ is based on the friction velocity U_τ and the channel half width $D/2$.

Profile of heat fluxes in fully developed channel flow with constant wall heat flux condition are plotted in Fig. 2 compared to the DNS of Kawamura[2004] and Durbin's second moment heat flux model. In this figure, EBE means the present elliptic blending model. Streamwise heat flux is globally well predicted by the present near wall models. However, it can be seen that the profiles of streamwise heat flux due to Durbin's model, which does not adopt any near wall model is largely under-predicted in comparison with the DNS.

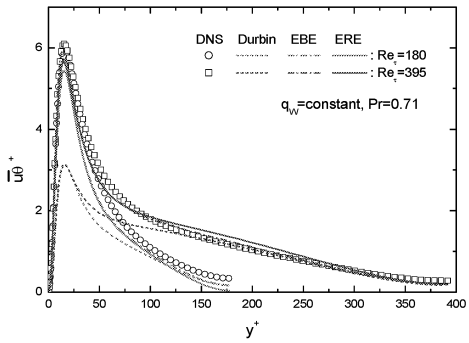

(a)

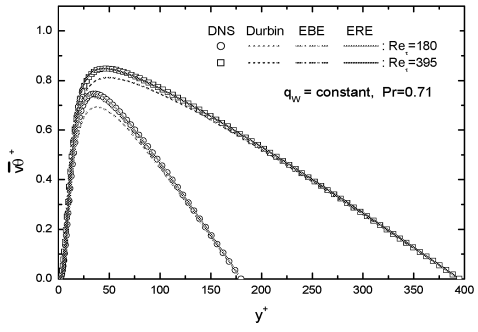

(b)

Fig. 2 Predicted heat transfer behaviour in a channel with constant wall heat flux boundary condition. symbols: DNS, lines: models. (a) Streamwise turbulent flux profiles, (b) Wall-normal turbulent heat flux profiles.

RESULTS AND DISCUSSIONS

Variation of heat transfer coefficients

Turbulent heat transfer of supercritical carbon dioxide flow in a square duct would be much different from that of normal state flow by the two respects. One is the strong secondary flow generated by the sharp density differentiation in the near wall region of the duct. The other is the buoyancy effect generated by density stratification on turbulence generation in the near wall region. During the gas cooling process of super-critical carbon dioxide, advanced increases in thermal conductivity. specific heat and density in the near wall region than those in the core region may enhance the heat transfer coefficient of the wall, while it operates to reduce the heat transfer coefficient during the gas heating process.

In the case of the first heat flux boundary condition, Fig. 3 shows that difference between heat transfer coefficients of upper and lower walls is negligible. However, as the flow approaches to pseudo-critical point, the heat transfer coefficients of upper wall become larger than those of lower wall. This is due to the buoyant generation of turbulence in the upper wall region and destruction in the lower wall region.

In the case of the second heat flux boundary condition, difference between heat transfer coefficient of upper and lower walls becomes significant as shown in Fig. 4.

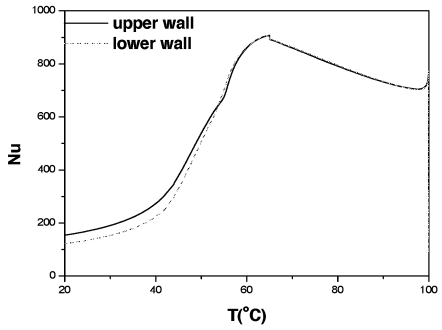

Fig. 3 Predicted heat transfer coefficient for the constant heat flux boundary condition for upper and lower walls only at $q = -40{,}000\,W/m^2$.

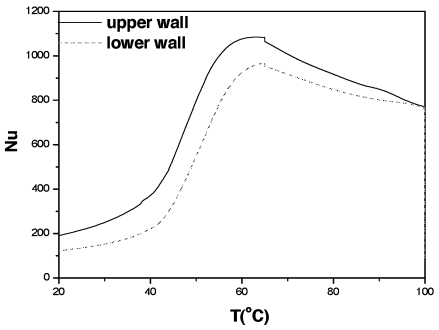

Fig. 4 Predicted heat transfer coefficient for the constant heat flux boundary condition for all around the duct wall at $q = -40{,}000\,W/m^2$.

During the heating or cooling processes of super-critical carbon dioxide flow in a duct, inhomogeneity of density between near wall and core

regions generates strong secondary motion as shown in Fig. 5 and Fig. 6. The secondary flow patterns are much changed according to the heat flux boundary conditions. In the case of constant heat flux condition for all around the wall, low density fluid generated near the side wall gives rise to strong downward fluid motion thereby inducing counter-clockwise vortex flow in the cross-sectional plane of the duct. This counter-clockwise vortex flow enhance the heat transfer of the upper wall region while weaken the heat transfer of the lower wall regions by moving the main stream from lower to upper parts. This moving of main stream from lower to upper parts make the gradients of streamwise velocity profiles steeper in the upper wall region than those in the lower wall region. However, in the case of adiabatic side wall and constant heat flux condition for upper and lower walls, the direction of secondary flow is reversed. In this case, the secondary motion is caused only by the density stratification in the upper and lower wall regions, so that the intensity of secondary motion is reduced compared to the case of all around constant heat flux boundary condition. Clockwise vortex flow moves the main stream from the upper to lower parts thereby enhancing the heat transfer of the lower wall while reducing the heat transfer of the upper wall.

During the gas cooling process of super-critical carbon dioxide flow in a duct, buoyant generation and destruction of turbulence. In the upper wall region, buoyancy destabilizes the flow to enhance turbulence, on the other hand in the lower wall region it stabilizes the flow to destruct turbulence. For the all around constant heat flux boundary condition, the secondary flow may operate productively with buoyant turbulent generation to enhance the heat transfer of upper wall region and to reduce the heat transfer of lower wall region. Difference in heat transfer coefficients between upper and lower walls is shown in Fig. 4 is caused by this mutal heat transfer fostering effect of secondary motion and buoyant turbulence generation. However, in the case of constant heat flux condition of only upper and lower walls, secondary flow and buoyant turbulent generation operate destructively so as to diminish the difference of heat transfer coefficient between upper and lower walls.

Fig.7 and Fig.8 show developments of Reynolds stresses $\overline{w^2}$, $\overline{v^2}$ in the upper and lower near wall regions. For the first heat flux boundary condition, $\overline{w^2}$, $\overline{v^2}$ of upper and lower wall regions have nearly same values at the high bulk mean temperature, however, as the cooling process is proceeded, $\overline{w^2}$, $\overline{v^2}$ of upper wall region increase slightly larger than those of lower wall region. It is due to the destabilizing effect of turbulence in the upper wall region while stabilizing effect in the lower wall region. In the case of second heat flux boundary condition, $\overline{w^2}$, $\overline{v^2}$ of upper wall region are always larger than those of lower wall region. This is due to the mutal heat transfer fostering effect of secondary flow and buoyant turbulence generation operate to enhance the heat transfer in upper region and reduce the heat transfer in lower wall region.

Present computations show that heat transfer phenomena of super-critical carbon dioxide in the horizontal square ducts are influenced significantly not only by magnitude of heat flux, but also the inhomogeneity of wall heat flux condition. These results indicate that reliable heat transfer coefficient correlation applicable to industry cannot be obtained by experimental means only. Large amount of computational works are needed to obtain the precise information on the effects of the inhomogeneity of heat flux boundary condition on the heat transfer of square ducts.

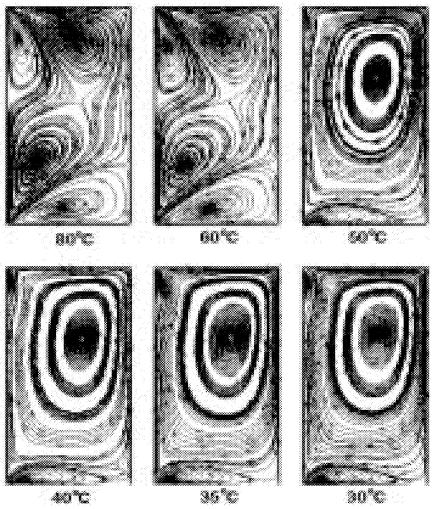

Fig. 5 Developing secondary flow patterns for the constant heat flux boundary condition of upper and lower walls and adiabatic condition of side wall

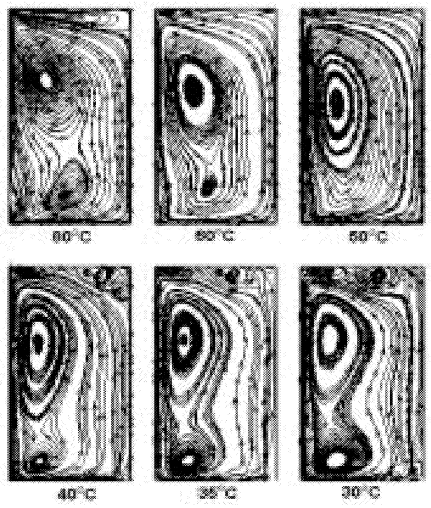

Fig. 6 Developing secondary flow patterns for constant heat flux boundary condition of all around the wall.

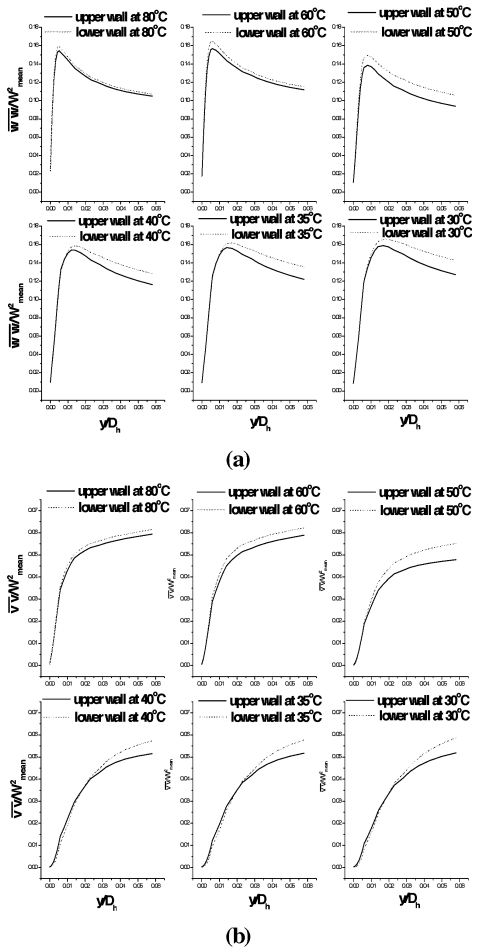

Fig. 7 Development of Reynolds stress profiles for the constant heat flux condition of upper and lower walls and adiabatic condition of side wall. (a) $\overline{w^2}$ (b) $\overline{v^2}$

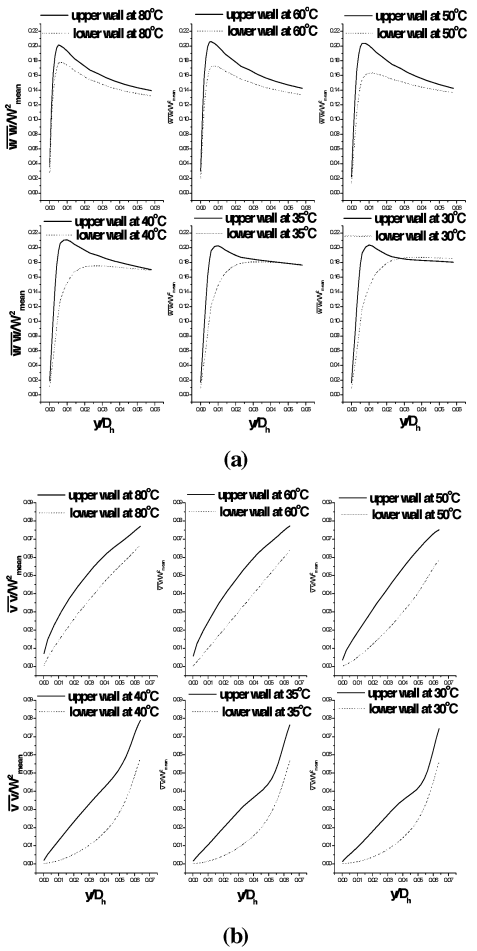

Fig. 8 Development of Reynolds stress profiles for the constant heat flux boundary condition of all around the wall. (a) $\overline{w^2}$ (b) $\overline{v^2}$

CONCLUSIONS

An elliptic-blending second moment closure is applied to the prediction of gas cooling process of turbulent super-critical carbon dioxide flow in a square duct. Computational results show that sharp differentiation of density between near wall and core regions generates strong secondary motion. The buoyant generation of turbulence, also takes important role in determining the heat transfer characteristics in the near wall regions. According to the heat flux boundary conditions, secondary flow patterns change significantly. In the case of constant heat flux boundary condition for all around the wall, mutal productive effect of secondary flow and buoyant generation of turbulence leads to increase the difference of heat transfer coefficients between upper and lower walls. On the other hand, in the case of constant heat flux condition for upper and lower walls but adiabatic condition for side wall, mutal destructive effect of secondary flow and buoyant generation of turbulence leads to diminish the difference of heat transfer coefficients between upper and lower walls.

Acknowledgment

This work was supported by Korea Science & Engineering Foundation(Grant No R01-2003-000-10571-0)

REFERENCES

Durbin, P.A., 1993, *J. Fluid Mech.*, Vol. 249, pp.465-498.

Kawamura, H, 2004, DNS database in "http://murasun.me.noda.tus.ac.jp/"

Krasnoshchekov, E. A. Kuraeva, I. V. and Profopopov, V. S., 1970, *Teplofizika Vysokikh Temperature*, Vol. 7, No. 5, pp. 922-930.

Lai, Y.G. and So, R.M.C., 1990, *Int. J. Heat Mass Transfer,* Vol. 33, pp. 1429-1440.

Petkhov, B. S., Krasnoshchekov, E. A. and Profopopov, V. S., 1961, *ASME International Developments in Heat Transfer* Part4: pp. 569-578.

Petrov, N. E., Propov, V. N., 1985, *Thermal Engineering*, Vol. 32, No. 3, pp. 131-134.

Pitla, S. S., Groll, E. A., and Ramadhyani, S., 2002, *International Journal of Refrigeration*, Vol. 22, pp. 887-895.

Thielen, L., Hanjalic, K. Jonker, H. and Manceau, R. 2004, submitted to Elsevier Science.